6 Kaon mixing

Authors: P. Dimopoulos, X. Feng, G. Herdoíza

The mixing of neutral pseudoscalar mesons plays an important role in the understanding of the physics of quark-flavour mixing and CP violation. In this section we discuss $K^0 - \bar{K}^0$ oscillations, which probe the physics of indirect CP violation. Extensive reviews on this subject can be found in Refs. [1–6]. With respect to the FLAG 19 report, in the new Sec. 6.2 of the present edition the reader will find an updated discussion regarding the lattice determination of the $K \to \pi\pi$ decay amplitudes and related quantities. Discussions concerning the kaon mixing within the Standard Model (SM) and Beyond the Standard Model (BSM) are presented in Secs. 6.3 and 6.4, respectively. We note that FLAG averages for SM and BSM bag parameters have not changed with respect to the FLAG 19 report.

6.1 Indirect CP violation and ϵ_K in the SM

Indirect CP violation arises in $K_L \to \pi\pi$ transitions through the decay of the CP $= +1$ component of K_L into two pions (which are also in a CP $= +1$ state). Its measure is defined as

$$\epsilon_K \;=\; \frac{\mathcal{A}[K_L \to (\pi\pi)_{I=0}]}{\mathcal{A}[K_S \to (\pi\pi)_{I=0}]}\,, \tag{130}$$

with the final state having total isospin zero. The parameter ϵ_K may also be expressed in terms of $K^0 - \bar{K}^0$ oscillations. In the Standard Model, ϵ_K receives contributions from: (i) short-distance (SD) physics given by $\Delta S = 2$ "box diagrams" involving $W^\pm$ bosons and u, c and t quarks; (ii) the long-distance (LD) physics from light hadrons contributing to the imaginary part of the dispersive amplitude M_{12} used in the two component description of $K^0 - \bar{K}^0$ mixing; (iii) the imaginary part of the absorptive amplitude Γ_{12} from $K^0 - \bar{K}^0$ mixing; and (iv) $\mathrm{Im}(A_0)/\mathrm{Re}(A_0)$, where A_0 is the $K \to (\pi\pi)_{I=0}$ decay amplitude. The various factors in this decomposition can vary with phase conventions. In terms of the $\Delta S = 2$ effective Hamiltonian, $\mathcal{H}_{\mathrm{eff}}^{\Delta S=2}$, it is common to represent contribution (i) by

$$\mathrm{Im}(M_{12}^{\mathrm{SD}}) \equiv \frac{1}{2m_K}\mathrm{Im}[\langle \bar{K}^0|\mathcal{H}_{\mathrm{eff}}^{\Delta S=2}|K^0\rangle], \tag{131}$$

and contribution (ii) by $\mathrm{Im}\,(M_{12}^{\mathrm{LD}})$. Contribution (iii) can be related to $\mathrm{Im}(A_0)/\mathrm{Re}(A_0)$ since $(\pi\pi)_{I=0}$ states provide the dominant contribution to absorptive part of the integral in Γ_{12}. Collecting the various pieces yields the following expression for the ϵ_K factor [5, 7–10]

$$\epsilon_K \;=\; \exp(i\phi_\epsilon)\,\sin(\phi_\epsilon)\left[\frac{\mathrm{Im}(M_{12}^{\mathrm{SD}})}{\Delta M_K} + \frac{\mathrm{Im}(M_{12}^{\mathrm{LD}})}{\Delta M_K} + \frac{\mathrm{Im}(A_0)}{\mathrm{Re}(A_0)}\right], \tag{132}$$

where the phase of ϵ_K is given by

$$\phi_\epsilon \;=\; \arctan\frac{\Delta M_K}{\Delta\Gamma_K/2}\,. \tag{133}$$

The quantities ΔM_K and $\Delta\Gamma_K$ are the mass and decay width differences between long- and short-lived neutral kaons. The experimentally known values of the above quantities read [11]:

$$|\epsilon_K| = 2.228(11)\times 10^{-3}\ , \tag{134}$$
$$\phi_\epsilon = 43.52(5)^\circ\ , \tag{135}$$
$$\Delta M_K \equiv M_{K_L} - M_{K_S} = 3.484(6)\times 10^{-12}\,\text{MeV}\ , \tag{136}$$
$$\Delta\Gamma_K \equiv \Gamma_{K_S} - \Gamma_{K_L} = 7.3382(33)\times 10^{-12}\,\text{MeV}\ , \tag{137}$$

where the latter three measurements have been obtained by imposing CPT symmetry.

We will start by discussing the short-distance effects (i) since they provide the dominant contribution to ϵ_K. To lowest order in the electroweak theory, the contribution to $K^0-\bar{K}^0$ oscillations arises from the so-called box diagrams, in which two W bosons and two "up-type" quarks (i.e., up, charm, top) are exchanged between the constituent down and strange quarks of the K mesons. The loop integration of the box diagrams can be performed exactly. In the limit of vanishing external momenta and external quark masses, the result can be identified with an effective four-fermion interaction, expressed in terms of the effective Hamiltonian

$$\mathcal{H}_{\text{eff}}^{\Delta S=2} = \frac{G_F^2 M_{\text{W}}^2}{16\pi^2}\mathcal{F}^0 Q^{\Delta S=2} + \text{h.c.}\ . \tag{138}$$

In this expression, G_F is the Fermi coupling, M_{W} the W-boson mass, and

$$Q^{\Delta S=2} = [\bar{s}\gamma_\mu(1-\gamma_5)d]\,[\bar{s}\gamma_\mu(1-\gamma_5)d] \equiv O_{\text{VV+AA}} - O_{\text{VA+AV}}\ , \tag{139}$$

is a dimension-six, four-fermion operator. The subscripts V and A denote vector ($\bar{s}\gamma_\mu d$) and axial-vector ($\bar{s}\gamma_\mu\gamma_5 d$) bilinears, respectively. The function $\mathcal{F}^0$ is given by

$$\mathcal{F}^0 = \lambda_c^2 S_0(x_c) + \lambda_t^2 S_0(x_t) + 2\lambda_c\lambda_t S_0(x_c,x_t)\ , \tag{140}$$

where $\lambda_a = V_{as}^* V_{ad}$, and $a = c\,,t$ denotes a flavour index. The quantities $S_0(x_c)$, $S_0(x_t)$ and $S_0(x_c,x_t)$ with $x_c = m_c^2/M_{\text{W}}^2$, $x_t = m_t^2/M_{\text{W}}^2$ are the Inami-Lim functions [12], which express the basic electroweak loop contributions without QCD corrections. The contribution of the up quark, which is taken to be massless in this approach, has been taken into account by imposing the unitarity constraint $\lambda_u + \lambda_c + \lambda_t = 0$.

When strong interactions are included, $\Delta S = 2$ transitions can no longer be discussed at the quark level. Instead, the effective Hamiltonian must be considered between mesonic initial and final states. Since the strong coupling is large at typical hadronic scales, the resulting weak matrix element cannot be calculated in perturbation theory. The operator product expansion (OPE) does, however, factorize long- and short- distance effects. For energy scales below the charm threshold, the $K^0-\bar{K}^0$ transition amplitude of the effective Hamiltonian can be expressed as

$$\langle\bar{K}^0|\mathcal{H}_{\text{eff}}^{\Delta S=2}|K^0\rangle = \frac{G_F^2 M_{\text{W}}^2}{16\pi^2}\Big[\lambda_c^2 S_0(x_c)\eta_1 + \lambda_t^2 S_0(x_t)\eta_2 + 2\lambda_c\lambda_t S_0(x_c,x_t)\eta_3\Big]$$
$$\times\left(\frac{\bar{g}(\mu)^2}{4\pi}\right)^{-\gamma_0/(2\beta_0)}\exp\left\{\int_0^{\bar{g}(\mu)} dg\left(\frac{\gamma(g)}{\beta(g)} + \frac{\gamma_0}{\beta_0 g}\right)\right\}\langle\bar{K}^0|Q_{\text{R}}^{\Delta S=2}(\mu)|K^0\rangle + \text{h.c.}\ , \tag{141}$$

where $\bar{g}(\mu)$ and $Q_{\text{R}}^{\Delta S=2}(\mu)$ are the renormalized gauge coupling and four-fermion operator in some renormalization scheme. The factors η_1, η_2 and η_3 depend on the renormalized coupling

$\bar{g}$, evaluated at the various flavour thresholds m_t, m_b, m_c and $M_{\rm W}$, as required by the OPE and Renormalization-Group (RG) running procedure that separate high- and low-energy contributions. Explicit expressions can be found in Refs. [4] and references therein, except that η_1 and η_3 have been calculated to NNLO in Refs. [13] and [14], respectively. We follow the same conventions for the RG equations as in Ref. [4]. Thus the Callan-Symanzik function and the anomalous dimension $\gamma(\bar{g})$ of $Q^{\Delta S=2}$ are defined by

$$\frac{d\bar{g}}{d\ln\mu} = \beta(\bar{g})\,, \qquad \frac{dQ_{\rm R}^{\Delta S=2}}{d\ln\mu} = -\gamma(\bar{g})\,Q_{\rm R}^{\Delta S=2}\,, \tag{142}$$

with perturbative expansions

$$\begin{aligned} \beta(g) &= -\beta_0\frac{g^3}{(4\pi)^2} - \beta_1\frac{g^5}{(4\pi)^4} - \cdots\,, \\ \gamma(g) &= \gamma_0\frac{g^2}{(4\pi)^2} + \gamma_1\frac{g^4}{(4\pi)^4} + \cdots\,. \end{aligned} \tag{143}$$

We stress that β_0, β_1 and γ_0 are universal, i.e., scheme independent. As for $K^0-\bar{K}^0$ mixing, this is usually considered in the naive dimensional regularization (NDR) scheme of $\overline{\rm MS}$, and below we specify the perturbative coefficient γ_1 in that scheme:

$$\begin{aligned} \beta_0 &= \left\{\frac{11}{3}N - \frac{2}{3}N_f\right\}, \qquad \beta_1 = \left\{\frac{34}{3}N^2 - N_f\left(\frac{13}{3}N - \frac{1}{N}\right)\right\}, \\ \gamma_0 &= \frac{6(N-1)}{N}, \qquad \gamma_1 = \frac{N-1}{2N}\left\{-21 + \frac{57}{N} - \frac{19}{3}N + \frac{4}{3}N_f\right\}. \end{aligned} \tag{144}$$

Note that for QCD the above expressions must be evaluated for $N = 3$ colours, while N_f denotes the number of active quark flavours. As already stated, Eq. (141) is valid at scales below the charm threshold, after all heavier flavours have been integrated out, i.e., $N_f = 3$.

In Eq. (141), the terms proportional to η_1, η_2 and η_3, multiplied by the contributions containing $\bar{g}(\mu)^2$, correspond to the Wilson coefficient of the OPE, computed in perturbation theory. Its dependence on the renormalization scheme and scale μ is canceled by that of the weak matrix element $\langle\bar{K}^0|Q_{\rm R}^{\Delta S=2}(\mu)|K^0\rangle$. The latter corresponds to the long-distance effects of the effective Hamiltonian and must be computed nonperturbatively. For historical, as well as technical reasons, it is convenient to express it in terms of the B-parameter B_K, defined as

$$B_K(\mu) = \frac{\left\langle\bar{K}^0\left|Q_{\rm R}^{\Delta S=2}(\mu)\right|K^0\right\rangle}{\frac{8}{3}f_K^2 m_K^2}\,. \tag{145}$$

The four-quark operator $Q^{\Delta S=2}(\mu)$ is renormalized at scale μ in some regularization scheme, for instance, NDR-$\overline{\rm MS}$. Assuming that $B_K(\mu)$ and the anomalous dimension $\gamma(g)$ are both known in that scheme, the renormalization group independent (RGI) B-parameter $\hat{B}_K$ is related to $B_K(\mu)$ by the exact formula

$$\hat{B}_K = \left(\frac{\bar{g}(\mu)^2}{4\pi}\right)^{-\gamma_0/(2\beta_0)} \exp\left\{\int_0^{\bar{g}(\mu)} dg\left(\frac{\gamma(g)}{\beta(g)} + \frac{\gamma_0}{\beta_0 g}\right)\right\} B_K(\mu)\,. \tag{146}$$

At NLO in perturbation theory the above reduces to

$$\hat{B}_K = \left(\frac{\bar{g}(\mu)^2}{4\pi}\right)^{-\gamma_0/(2\beta_0)} \left\{1 + \frac{\bar{g}(\mu)^2}{(4\pi)^2}\left[\frac{\beta_1\gamma_0 - \beta_0\gamma_1}{2\beta_0^2}\right]\right\} B_K(\mu)\,. \tag{147}$$

To this order, this is the scale-independent product of all μ-dependent quantities in Eq. (141).

Lattice-QCD calculations provide results for $B_K(\mu)$. However, these results are usually obtained in intermediate schemes other than the continuum $\overline{\rm MS}$ scheme used to calculate the Wilson coefficients appearing in Eq. (141). Examples of intermediate schemes are the RI/MOM scheme [15] (also dubbed the "Rome-Southampton method") and the Schrödinger functional (SF) scheme [16]. These schemes are used as they allow a nonperturbative renormalization of the four-fermion operator, using an auxiliary lattice simulation. This allows $B_K(\mu)$ to be calculated with percent-level accuracy, as described below.

In order to make contact with phenomenology, however, and in particular to use the results presented above, one must convert from the intermediate scheme to the $\overline{\rm MS}$ scheme or to the RGI quantity $\hat{B}_K$. This conversion relies on 1- or 2-loop perturbative matching calculations, the truncation errors in which are, for many recent calculations, the dominant source of error in $\hat{B}_K$ (see, for instance, Refs. [17–21]). While this scheme-conversion error is not, strictly speaking, an error of the lattice calculation itself, it must be included in results for the quantities of phenomenological interest, namely, $B_K(\overline{\rm MS}, 2\,{\rm GeV})$ and $\hat{B}_K$. Incidentally, we remark that this truncation error is estimated in different ways and that its relative contribution to the total error can considerably differ among the various lattice calculations. We note that this error can be minimized by matching between the intermediate scheme and $\overline{\rm MS}$ at as large a scale μ as possible (so that the coupling which determines the rate of convergence is minimized). Recent calculations have pushed the matching μ up to the range $3 - 3.5\,{\rm GeV}$. This is possible because of the use of nonperturbative RG running determined on the lattice [18, 20, 22]. The Schrödinger functional offers the possibility to run nonperturbatively to scales $\mu \sim M_{\rm W}$ where the truncation error can be safely neglected. However, so far this has been applied only for two flavours for B_K in Ref. [23] and for the case of the BSM bag parameters in Ref. [24], see more details in Sec. 6.4.

Perturbative truncation errors in Eq. (141) also affect the Wilson coefficients η_1, η_2 and η_3. It turns out that the largest uncertainty arises from the charm quark contribution $\eta_1 = 1.87(76)$ [13]. Although it is now calculated at NNLO, the series shows poor convergence. The net effect from the uncertainty on η_1 on the amplitude in Eq. (141) is larger than that of present lattice calculations of B_K. Exploiting an idea presented in Ref. [25], it has been recently shown in Ref. [26] that, by using the $u-t$ instead of the usual $c-t$ unitarity in the ϵ_K computation, the perturbative uncertainties associated with residual short-distance quark contributions can be reduced.

We will now proceed to discuss the remaining contributions to ϵ_K in Eq. (132). An analytical estimate of the leading contribution from $\mathrm{Im}(M_{12}^{\rm LD})$ based on χPT, shows that it is approximately proportional to $\xi \equiv \mathrm{Im}(A_0)/\mathrm{Re}(A_0)$ so that Eq. (132) can be written as follows [9, 10]

$$\epsilon_K \;=\; \exp(i\phi_\epsilon)\,\sin(\phi_\epsilon)\left[\frac{\mathrm{Im}(M_{12}^{\rm SD})}{\Delta M_K} \;+\; \rho\,\xi\right], \tag{148}$$

where the deviation of ρ from one parameterizes the long-distance effects in $\mathrm{Im}(M_{12})$.

In order to facilitate the subsequent discussions about the status of the lattice studies of $K \to \pi\pi$ and of the current estimates of ξ, we proceed by providing a brief account of the parameter ϵ' that describes direct CP-violation in the kaon sector. The definition of ϵ' is given by:

$$\epsilon' \equiv \frac{1}{\sqrt{2}}\frac{\mathcal{A}[K_S \to (\pi\pi)_{I=2}]}{\mathcal{A}[K_S \to (\pi\pi)_{I=0}]}\left(\frac{\mathcal{A}[K_L \to (\pi\pi)_{I=2}]}{\mathcal{A}[K_S \to (\pi\pi)_{I=2}]} - \frac{\mathcal{A}[K_L \to (\pi\pi)_{I=0}]}{\mathcal{A}[K_S \to (\pi\pi)_{I=0}]}\right). \tag{149}$$

By selecting appropriate phase conventions for the mixing parameters between K^0 and $\bar{K}^0$ CP-eigenstates (see e.g. Ref. [2] for further details), the expression of ϵ' can be expressed in terms of the real and imaginary parts of the isospin amplitudes, as follows

$$\epsilon' \;=\; \frac{i\omega\, e^{i(\delta_2-\delta_0)}}{\sqrt{2}}\left[\frac{\mathrm{Im}(A_2)}{\mathrm{Re}(A_2)}-\xi\right], \tag{150}$$

where $\omega = \mathrm{Re}(A_2)/\mathrm{Re}(A_0)$, A_2 denotes the $\Delta I = 3/2$ $K \to \pi\pi$ decay amplitude, and δ_I denotes the strong scattering phase shifts in the corresponding, $I = 0, 2$, $K \to (\pi\pi)_I$ decays. Given that the phase, $\phi'_\epsilon = \delta_2 - \delta_0 + \pi/2 = 42.3(1.5)^\circ$ [11] is nearly equal to ϕ_ϵ in Eq. (135), the ratio of parameters characterizing the direct and indirect CP-violation in the kaon sector can be approximated in the following way,

$$\epsilon'/\epsilon \;\approx\; \mathrm{Re}(\epsilon'/\epsilon) \;=\; \frac{\omega}{\sqrt{2}\,|\epsilon_K|}\left[\frac{\mathrm{Im}(A_2)}{\mathrm{Re}(A_2)}-\xi\right], \tag{151}$$

where on the left hand side we have set $\epsilon \equiv \epsilon_K$. The experimentally measured value reads [11],

$$\mathrm{Re}(\epsilon'/\epsilon) = 16.6(2.3)\times 10^{-4}\,. \tag{152}$$

We remark that isospin breaking and electromagnetic effects (see Refs. [27, 28], and the discussion in Ref. [3]) introduce additional correction terms into Eq. (151).

6.2 Lattice-QCD studies of the $K \to (\pi\pi)_I$ decay amplitudes, ξ and ϵ'/ϵ

As a preamble to this section, it should be noted that the study of $K \to \pi\pi$ decay amplitudes requires the development of computational strategies that are at the forefront of lattice QCD techniques. These studies represent a significant advance in the study of kaon physics. However, at present, they have not yet reached the same level of maturity of most of the quantities analyzed in the FLAG report, where, for instance, independent results by various lattice collaborations are being compared and averaged. In the present version of this section we will therefore review the current status of $K \to \pi\pi$ lattice computations, but we will provide a FLAG average only for the case of the decay amplitude A_2.

We start by reviewing the determination of the parameter $\xi = \mathrm{Im}(A_0)/\mathrm{Re}(A_0)$. An estimate of ξ has been obtained from a direct evaluation of the ratio of amplitudes $\mathrm{Im}(A_0)/\mathrm{Re}(A_0)$ where $\mathrm{Im}(A_0)$ is determined from a lattice-QCD computation by RBC/UKQCD 20 [29] employing $N_f = 2+1$ Möbius domain wall fermions at a single value of the lattice spacing while $\mathrm{Re}(A_0) \simeq |A_0|$ and the value $|A_0| = 3.320(2)\times 10^{-7}$ GeV are used based on the relevant experimental input [11] from the decay to two pions. This leads to a result for ξ with a rather large relative error,

$$\xi = -2.1(5)\cdot 10^{-4}. \tag{153}$$

Following a similar procedure, an estimate of ξ was obtained through the use of a previous lattice QCD determination of $\mathrm{Im}(A_0)$ by RBC/UKQCD 15G [30]. We refer to Tab. 28 for further details about these computations of $\mathrm{Im}(A_0)$. The comparison of the estimates of ξ based on lattice QCD input are collected in Tab. 30.

Another estimate for ξ can be obtained through a lattice-QCD computation of the ratio of amplitudes $\mathrm{Im}(A_2)/\mathrm{Re}(A_2)$ by RBC/UKQCD 15F [31] where the continuum-limit result is based on computations at two values of the lattice spacing employing $N_f = 2+1$ Möbius

domain wall fermions. Further details about the lattice computations of A_2 are collected in Tab. 29. To obtain the value of ξ, the expression in Eq. (151) together with the experimental values of $\mathrm{Re}(\epsilon'/\epsilon)$, $|\epsilon_K|$ and ω are used. In this case we obtain $\xi = -1.6(2)\cdot 10^{-4}$. The use of the updated value of $\mathrm{Im}(A_2) = -8.34(1.03)\times 10^{-13}\,\mathrm{GeV}$ from Ref. [29],[1] in combination with the experimental value of $\mathrm{Re}(A_2) = 1.479(4)\times 10^{-8}\,\mathrm{GeV}$, introduces a small change with respect to the above result. The value for ξ reads [2]

$$\xi = -1.7(2)\cdot 10^{-4}. \tag{154}$$

A phenomenological estimate can also be obtained from the relationship of ξ to $\mathrm{Re}(\epsilon'/\epsilon)$, using the experimental value of the latter and further assumptions concerning the estimate of hadronic contributions. The corresponding value of ξ reads [9, 10]

$$\xi = -6.0(1.5)\cdot 10^{-2}\sqrt{2}\,|\epsilon_K| = -1.9(5)\cdot 10^{-4}. \tag{155}$$

We note that the use of the experimental value for $\mathrm{Re}(\epsilon'/\epsilon)$ is based on the assumption that it is free from New Physics contributions. The value of ξ can then be combined with a χPT-based estimate for the long-range contribution, $\rho = 0.6(3)$ [10]. Overall, the combination $\rho\xi$ appearing in Eq. (148) leads to a suppression of the SM prediction of $|\epsilon_K|$ by about 3(2)% relative to the experimental measurement of $|\epsilon_K|$ given in Eq. (134), regardless of whether the phenomenological estimate of ξ [see Eq. (155)] or the most precise lattice result [see Eq. (153)] are used. The uncertainty in the suppression factor is dominated by the error on ρ. Although this is a small correction, we note that its contribution to the error of ϵ_K is larger than that arising from the value of B_K reported below.

Efforts are under way to compute the long-distance contributions to ϵ_K [33] and to the $K_L - K_S$ mass difference in lattice QCD [25, 34–36]. However, the results are not yet precise enough to improve the accuracy in the determination of the parameter ρ.

The lattice-QCD study of $K \to \pi\pi$ decays provides crucial input to the SM prediction of ϵ_K. We now proceed to describe the current status of these computations. In recent years, the RBC/UKQCD collaboration has undertaken a series of lattice-QCD calculations of $K \to \pi\pi$ decay amplitudes [29–31]. In 2015, the first calculation of the $K \to (\pi\pi)_{I=0}$ decay amplitude A_0 was performed using physical kinematics on a $32^3 \times 64$ lattice with an inverse lattice spacing of $a^{-1} = 1.3784(68)$ GeV [30, 37]. The main features of the RBC/UKQCD 15G calculation included, fixing the $I = 0$ $\pi\pi$ energy very close to the kaon mass by imposing G-parity boundary conditions, a continuum-like operator mixing pattern through the use of a domain wall fermion action with accurate chiral symmetry, and the construction of the complete set of correlation functions by computing seventy-five distinct diagrams. Results for the real and the imaginary parts of the decay amplitude A_0 from the RBC/UKQCD 15G computation are collected in Tab. 28, where the first error is statistical and the second one is systematic.

[1] The update in $\mathrm{Im}(A_2)$ is due to a change in the value of the imaginary part of the ratio of CKM matrix elements, $\tau = -V_{ts}^* V_{td}/V_{us}^* V_{ud}$, as given in Ref. [32]. The lattice QCD input is therefore the one reported in Ref. [31].

[2] The current estimates for the corrections owing to isospin breaking and electromagnetic effects [28] imply a relative change on the theoretical value for ϵ'/ϵ by about -20% with respect to the determination based on Eq. (151). The size of these isospin breaking and electromagnetic corrections is related to the enhancement of the decay amplitudes between the $I = 0$ and the $I = 2$ channels. As a consequence, one obtains a similar reduction on ξ, leading to a value that is close to the result of Eq. (153).

Collaboration	Ref.	N_f	publication status	continuum extrapolation	chiral extrapolation	finite volume	renormalization	running/matching	$\mathrm{Re}(A_0)$ $[10^{-7}\ \mathrm{GeV}]$	$\mathrm{Im}(A_0)$ $[10^{-11}\ \mathrm{GeV}]$
RBC/UKQCD 20	[29]	2+1	A	■	○	○	★	*a*	2.99(0.32)(0.59)	−6.98(0.62)(1.44)
RBC/UKQCD 15G	[30]	2+1	A	■	○	○	★	*b*	4.66(1.00)(1.26)	−1.90(1.23)(1.08)

a Nonperturbative renormalization with the RI/SMOM scheme at a scale of 1.53 GeV and running to 4.01 GeV employing a nonperturbatively determined step-scaling function. Conversion to $\overline{\mathrm{MS}}$ at 1-loop order.

b Nonperturbative renormalization with the RI/SMOM scheme at a scale of 1.53 GeV. Conversion to $\overline{\mathrm{MS}}$ at 1-loop order.

Table 28: Results for the real and imaginary parts of the $K \to \pi\pi$ decay amplitude A_0 from lattice-QCD computations with $N_f = 2 + 1$ dynamical flavours. Information about the renormalization, running and matching to the $\overline{\mathrm{MS}}$ scheme is indicated in the column "running/matching", with details given at the bottom of the table. We refer to the text for further details about the main differences between the lattice computations in Refs. [29] and [30].

The latest 2020 calculation RBC/UKQCD 20 [29] using the same lattice setup has improved the 2015 calculation RBC/UKQCD 15G [30] in three important aspects: (i) an increase by a factor of 3.4 in statistics; (ii) the inclusion of a scalar two-quark operator and the addition of another pion-pion operator to isolate the ground state, and (iii) the use of step scaling techniques to raise the renormalization scale from 1.53 GeV to 4.01 GeV. The updated determinations of the real and the imaginary parts of A_0 in Ref. [29] are shown in Tab. 28.

As previously discussed, the determination of $\mathrm{Im}(A_0)$ from Ref. [29] has been used to obtain the value of the parameter ξ in Eq. (153). A first-principles computation of $\mathrm{Re}(A_0)$ is essential to address the so-called $\Delta I = 1/2$ puzzle associated to the enhancement of $\Delta I = 1/2$ over $\Delta I = 3/2$ transitions owing, crucially, to long distance effects. Indeed, short-distance enhancements in the Wilson coefficients are not large enough to explain the $\Delta I = 1/2$ rule [38, 39]. Lattice-QCD calculations do provide a method to study such a long-distance enhancement. The combination of the result for A_0 in Tab. 28 with the earlier lattice calculation of A_2 in Ref. [31] leads to the ratio, $\mathrm{Re}(A_0)/\mathrm{Re}(A_2) = 19.9(5.0)$, which agrees with the experimentally measured value, $\mathrm{Re}(A_0)/\mathrm{Re}(A_2) = 22.45(6)$. In Ref. [29], the lattice determination of relative size of direct CP violation was updated as follows,

$$\mathrm{Re}(\epsilon'/\epsilon) = 21.7(2.6)(6.2)(5.0) \times 10^{-4}, \tag{156}$$

where the first two errors are statistical and systematic, respectively. The third error arises from the omitted strong and electromagnetic isospin breaking effects. The value of $\mathrm{Re}(\epsilon'/\epsilon)$ in Eq. (156) uses the experimental values of $\mathrm{Re}(A_0)$ and $\mathrm{Re}(A_2)$. The lattice determination of $\mathrm{Re}(\epsilon'/\epsilon)$ is in good agreement with the experimental result in Eq. (152). However, while the

Collaboration	Ref.	N_f	publication status	continuum extrapolation	chiral extrapolation	finite volume	renormalization	running/matching	$\mathrm{Re}(A_2)$ $[10^{-8}\ \mathrm{GeV}]$	$\mathrm{Im}(A_2)$ $[10^{-13}\ \mathrm{GeV}]$
RBC/UKQCD 15F	[31]	2+1	A	○	○	★	★	a	1.50(0.04)(0.14)	$-8.34(1.03)^{\diamond}$

a Nonperturbative renormalization with the RI/SMOM scheme at a scale of 3 GeV. Conversion to $\overline{\mathrm{MS}}$ at 1-loop order.

$^{\diamond}$ This value of $\mathrm{Im}(A_2)$ is an update reported in Ref. [29] which is based on the lattice QCD computation in Ref. [31] but where a change in the value of the imaginary part of the ratio of CKM matrix elements $\tau = -V_{ts}^* V_{td} / V_{us}^* V_{ud}$ reported in Ref. [32] has been applied.

Table 29: Results for the real and the imaginary parts of the $K \to \pi\pi$ decay amplitude A_2 from lattice-QCD computations with $N_f = 2+1$ dynamical flavours. Information about the renormalization and matching to the $\overline{\mathrm{MS}}$ scheme is indicated in the column "running/matching", with details given at the bottom of the table.

Collaboration	Ref.	N_f	ξ
RBC/UKQCD 20†	[29]	2+1	$-2.1(5)\cdot 10^{-4}$
RBC/UKQCD 15G$^{\diamond}$	[30]	2+1	$-0.6(5)\cdot 10^{-4}$
RBC/UKQCD 15F*	[31]	2+1	$-1.7(2)\cdot 10^{-4}$

† Estimate for ξ obtained from a direct evaluation of the ratio of amplitudes $\mathrm{Im}(A_0)/\mathrm{Re}(A_0)$ where $\mathrm{Im}(A_0)$ is determined from the lattice-QCD computation of Ref. [29] while for $\mathrm{Re}(A_0) \simeq |A_0|$ is taken from the experimental value for $|A_0|$.

$^{\diamond}$ Estimate for ξ obtained from a direct evaluation of the ratio of amplitudes $\mathrm{Im}(A_0)/\mathrm{Re}(A_0)$ where $\mathrm{Im}(A_0)$ is determined from the lattice-QCD computation of Ref. [30] while for $\mathrm{Re}(A_0) \simeq |A_0|$ is taken from the experimental value for $|A_0|$.

* Estimate for ξ based on the use of Eq. (151). The new value of $\mathrm{Im}(A_2)$ reported in Ref. [29]—based on the lattice-QCD computation of Ref. [31] following an update of a nonlattice input—is used in combination with the experimental values for $\mathrm{Re}(A_2)$, $\mathrm{Re}(\epsilon'/\epsilon)$, $|\epsilon_K|$ and ω.

Table 30: Results for the parameter $\xi = \mathrm{Im}(A_0)/\mathrm{Re}(A_0)$ obtained through the combination of lattice-QCD determinations of $K \to \pi\pi$ decay amplitudes with $N_f = 2+1$ dynamical flavours and experimental inputs.

result in Eq. (156) represents a significant step forward, it is important to keep in mind that the calculation of A_0 is currently based on a single value of the lattice spacing. It is expected that future work with additional values of the lattice spacing will contribute to improve the

precision. For a description of the computation of the $\pi\pi$ scattering phase shifts entering in the determination of $\mathrm{Re}(\epsilon'/\epsilon)$ in Eq. (156), we refer to Ref. [40].

The real and imaginary values of the amplitude A_2 have been determined by RBC/UKQCD 15F [31] employing $N_f = 2+1$ Möbius domain wall fermions at two values of the lattice spacing, namely $a = 0.114\,\mathrm{fm}$ and $0.083\,\mathrm{fm}$, and performing simulations at the physical pion mass with $M_\pi L \approx 3.8$.

A compilation of lattice results for the real and imaginary parts of the $K \to \pi\pi$ decay amplitudes, A_0 and A_2, with $N_f = 2+1$ flavours of dynamical quarks is shown in Tabs. 28 and 29. In Appendix C.4.1 we collect the corresponding information about the lattice QCD simulations, including the values of some of the most relevant parameters. The results for the parameter ξ, determined through the combined use of $K \to \pi\pi$ amplitudes computed on the lattice and experimental inputs, are presented in Tab. 30. As previously discussed, we remark that the total uncertainty on the reported values of ξ depends on the specific way in which the lattice and experimental inputs are selected.

The determination of the real and imaginary parts of A_2 by RBC/UKQCD 15F shown in Tab. 29 is free of red tags. We therefore quote the following FLAG averages:

$$N_f = 2+1: \qquad \begin{aligned} \mathrm{Re}(A_2) &= 1.50(0.04)(0.14) \times 10^{-8}\ \mathrm{GeV}, \\ \mathrm{Im}(A_2) &= -8.34(1.03) \times 10^{-13}\ \mathrm{GeV}, \end{aligned} \qquad \text{Ref. [31].} \tag{157}$$

Besides the RBC/UKQCD collaboration programme [29–31] using domain-wall fermions, an approach based on improved Wilson fermions [41, 42] has presented a determination of the $K \to \pi\pi$ decay amplitudes, A_0 and A_2, at unphysical quark masses. For an analysis of the scaling with the number of colours of $K \to \pi\pi$ decay amplitudes using lattice-QCD computations, we refer to Refs. [43, 44].

Recent proposals aiming at the inclusion of electromagnetism in lattice-QCD calculations of $K \to \pi\pi$ decays are being explored [45, 46] in order to reduce the uncertainties associated with isospin breaking effects.

Finally, we notice that ϵ_K receives a contribution from $|V_{cb}|$ through the λ_t parameter in Eq. (140). The present uncertainty on $|V_{cb}|$ has a significant impact on the error of ϵ_K (see, e.g., Refs. [47, 48] and the recent update in Ref. [49]).

6.3 Lattice computation of B_K

Lattice calculations of B_K are affected by the same type of systematic effects discussed in previous sections of this review. However, the issue of renormalization merits special attention. The reason is that the multiplicative renormalizability of the relevant operator $Q^{\Delta S=2}$ is lost once the regularized QCD action ceases to be invariant under chiral transformations. As a result, the renormalization pattern of B_K depends on the specific choice of the fermionic discretization.

In the case of Wilson fermions, $Q^{\Delta S=2}$ mixes with four additional dimension-six operators, which belong to different representations of the chiral group, with mixing coefficients that are finite functions of the gauge coupling. This complicated renormalization pattern was identified as the main source of systematic error in earlier, mostly quenched calculations of B_K with Wilson quarks. It can be bypassed via the implementation of specifically designed methods, which are either based on Ward identities [50] or on a modification of the Wilson quark action, known as twisted-mass QCD [51–53].

An advantage of staggered fermions is the presence of a remnant $U(1)$ chiral symmetry. However, at nonvanishing lattice spacing, the symmetry among the extra unphysical degrees of freedom (tastes) is broken. As a result, mixing with other dimension-six operators cannot be avoided in the staggered formulation, which complicates the determination of the B-parameter. In general, taste conserving mixings are implemented directly in the lattice computation of the matrix element. The effects of the broken taste symmetry are usually treated through an effective field theory, staggered Chiral Perturbation Theory (SχPT) [54, 55], parameterizing the quark-mass and lattice-spacing dependences.

Fermionic lattice actions based on the Ginsparg-Wilson relation [56] are invariant under the chiral group, and hence four-quark operators such as $Q^{\Delta S=2}$ renormalize multiplicatively. However, depending on the particular formulation of Ginsparg-Wilson fermions, residual chiral symmetry breaking effects may be present in actual calculations. For instance, in the case of domain-wall fermions, the finiteness of the extra 5th dimension implies that the decoupling of modes with different chirality is not exact, which produces a residual nonzero quark mass in the chiral limit. The mixing with dimension-six operators of different chirality is expected to be an $\mathcal{O}(m_{\rm res}^2)$ suppressed effect [57, 58] that should be investigated on a case-by-case basis.

Before proceeding to the description and compilation of the results of B_K, we would like to reiterate a discussion presented in the previous FLAG report about an issue related to the computation of the kaon bag parameters through lattice-QCD simulations with $N_f = 2+1+1$ dynamical quarks. In practice, this only concerns the calculations of the kaon B-parameters including dynamical charm-quark effects in Ref. [59], that were examined in the FLAG 16 report. As described in Sec. 6.1, the effective Hamiltonian in Eq. (138) depends solely on the operator $Q^{\Delta S=2}$ in Eq. (139) —which appears in the definition of B_K in Eq. (145)— at energy scales below the charm threshold where charm-quark contributions are absent. As a result, a computation of B_K based on $N_f = 2+1+1$ dynamical simulations will include an extra sea-quark contribution from charm-quark loop effects for which there is at present no direct evaluation in the literature.

When the matrix element of $Q^{\Delta S=2}$ is evaluated in a theory that contains a dynamical charm quark, the resulting estimate for B_K must then be matched to the three-flavour theory that underlies the effective four-quark interaction.[3] In general, the matching of $2+1$-flavour QCD with the theory containing $2+1+1$ flavours of sea quarks is performed around the charm threshold. It is usually accomplished by requiring that the coupling and quark masses are equal in the two theories at a renormalization scale μ around m_c. In addition, B_K should be renormalized and run, in the four-flavour theory, to the value of μ at which the two theories are matched, as described in Sec. 6.1. The corrections associated with this matching are of order $(E/m_c)^2$, where E is a typical energy in the process under study, since the subleading operators have dimension eight [60].

When the kaon-mixing amplitude is considered, the matching also involves the relation between the relevant box diagrams and the effective four-quark operator. In this case, corrections of order $(E/m_c)^2$ arise not only from the charm quarks in the sea, but also from the valence sector, since the charm quark propagates in the box diagrams. We note that the original derivation of the effective four-quark interaction is valid up to corrections of order $(E/m_c)^2$. The kaon-mixing amplitudes evaluated in the $N_f = 2+1$ and $2+1+1$ theories are thus subject to corrections of the same order in E/m_c as the derivation of the conventional four-quark interaction.

[3] We thank Martin Lüscher for an interesting discussion on this issue.

Regarding perturbative QCD corrections at the scale of the charm-quark mass on the amplitude in Eq. (141), the uncertainty on η_1 and η_3 factors is of $\mathcal{O}(\alpha_s(m_c)^3)$ [13, 14], while that on η_2 is of $\mathcal{O}(\alpha_s(m_c)^2)$ [61]. [4] On the other hand, the corrections of order $(E/m_c)^2$ due to dynamical charm-quark effects in the matching of the amplitudes are further suppressed by powers of $\alpha_s(m_c)$ and by a factor of $1/N_c$, given that they arise from quark-loop diagrams. In order to make progress in resolving this so far uncontrolled systematic uncertainty, it is essential that any future calculation of B_K with $N_f = 2+1+1$ flavours properly addresses the size of these residual dynamical charm effects in a quantitative way.

Another issue in this context is how the lattice scale and the physical values of the quark masses are determined in the $2+1$ and $2+1+1$ flavour theories. Here it is important to consider in which way the quantities used to fix the bare parameters are affected by a dynamical charm quark.

A recent study [62] using three degenerate light quarks, together with a charm quark, indicates that the deviations between the $N_f = 3+1$ and the $N_f = 3$ theories are considerably below the 1% level in dimensionless quantities constructed from ratios of gradient flow observables, such as t_0 and w_0, used for scale setting. This study extends the nonperturbative investigations with two heavy mass-degenerate quarks [63, 64] which indicate that dynamical charm-quark effects in low-energy hadronic observables are considerably smaller than the expectation from a naive power counting in terms of $\alpha_s(m_c)$. For an additional discussion on this point, we refer to Ref. [59]. Given the hierarchy of scales between the charm-quark mass and that of B_K, we expect these errors to be modest, but a more quantitative understanding is needed as statistical errors on B_K are reduced. Within this review we will not discuss this issue further. However, we wish to point out that the present discussion also applies to $N_f = 2+1+1$ computations of the kaon BSM B-parameters discussed in Sec. 6.4.

A compilation of results for B_K with $N_f = 2, 2+1$ and $2+1+1$ flavours of dynamical quarks is shown in Tabs. 31 and 32, as well as Fig. 20. An overview of the quality of systematic error studies is represented by the colour coded entries in Tabs. 31 and 32. The values of the most relevant lattice parameters, and comparative tables on the various estimates of systematic errors have been collected in the corresponding Appendices of the previous FLAG editions [65–67].

Since the last edition of the FLAG report no new results for B_K have appeared in the bibliography. We mention here an ongoing work related to the B_K computation where the relevant operators are defined in the gradient flow framework. In a first publication [68] the small flow time expansion method is applied in order to compute, to 1-loop approximation, the finite matching coefficients between the gradient flow and the $\overline{\text{MS}}$ schemes for the operators entering the B_K computation.

For a detailed description of previous B_K calculations—and in particular those considered in the computation of the average values—we refer the reader to the FLAG 19 [65], FLAG 16 [66] and FLAG 13 [67] reports.

We now give the global averages for B_K for $N_f = 2+1+1, 2+1$ and 2 dynamical flavours. The details about the calculation of these averages can be found in FLAG 19 [65].

We begin with the $N_f = 2+1$ global average since it is estimated by employing four different B_K results, namely BMW 11 [22], Laiho 11 [17], RBC/UKQCD 14B [20] and SWME

[4] The recent results [26] based on the use of $u-t$ unitarity for the two corresponding perturbative factors, also have an uncertainty of $\mathcal{O}(\alpha_s(m_c)^2)$ and $\mathcal{O}(\alpha_s(m_c)^3)$. The estimates for the missing higher-order contributions are, however, expected to be reduced with respect to the more traditional case where $c-t$ unitarity is used.

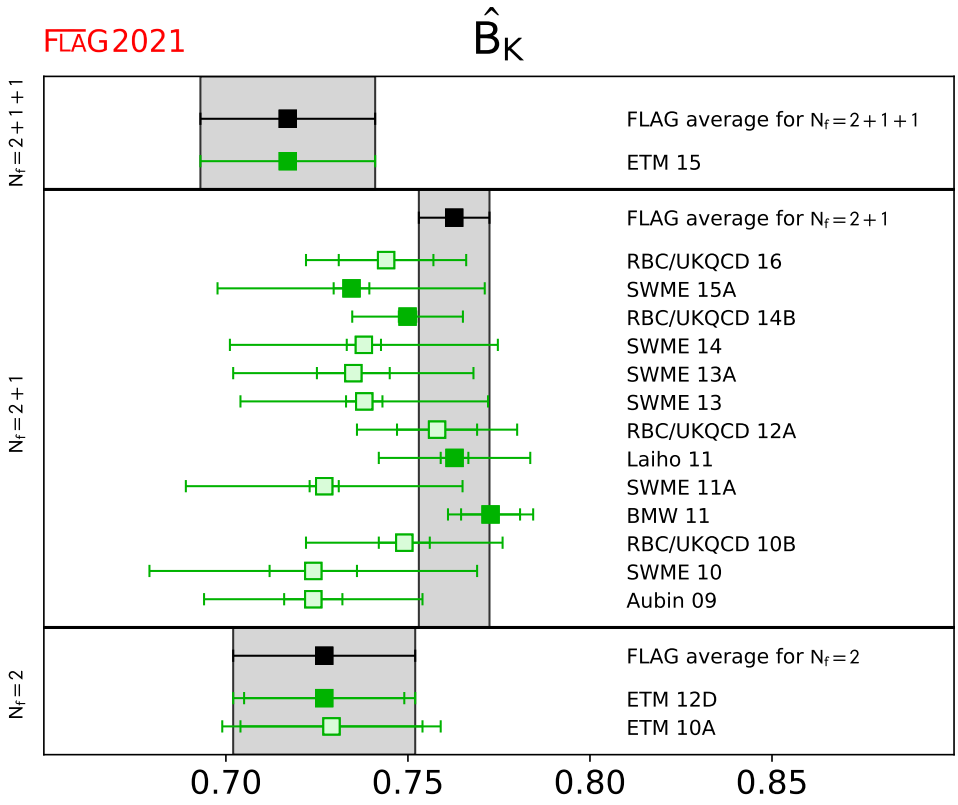

Figure 20: Recent unquenched lattice results for the RGI B-parameter $\hat{B}_K$. The grey bands indicate our global averages described in the text. For $N_f = 2+1+1$ and $N_f = 2$ the global averages coincide with the results by ETM 15 and ETM 12D, respectively.

15A [21]. Note also that the expression of ϵ_K in terms of B_K is obtained in the three-flavour theory (see Sec. 6.1). After constructing the global covariance matrix according to Schmelling [69], we arrive at:

$$N_f = 2+1: \qquad \hat{B}_K = 0.7625(97) \qquad \text{Refs. [17, 20–22]}, \tag{158}$$

with $\chi^2/\text{dof} = 0.675$. After applying the NLO conversion factor $\hat{B}_K/B_K^{\overline{\text{MS}}}(2\,\text{GeV}) = 1.369$,[5] this translates into

$$N_f = 2+1: \qquad B_K^{\overline{\text{MS}}}(2\,\text{GeV}) = 0.5570(71) \qquad \text{Refs. [17, 20–22]}. \tag{159}$$

Note that the statistical errors of each calculation entering the global average are small enough to make their results statistically incompatible. It is only because of the relatively large systematic errors that the weighted average produces a value of $\mathcal{O}(1)$ for the reduced χ^2.

There is only a single result for $N_f = 2+1+1$, computed by the ETM collaboration [59]. Since it is free of red tags, it qualifies as the currently best global average, i.e.,

$$N_f = 2+1+1: \quad \hat{B}_K = 0.717(18)(16)\,, \quad B_K^{\overline{\text{MS}}}(2\,\text{GeV}) = 0.524(13)(12) \quad \text{Ref. [59]}. \tag{160}$$

[5] We refer to the FLAG 19 report [65] for a discussion about the estimates of these conversion factors.

For $N_f = 2$ flavours the best global average is given by a single result, that of ETM 12D [70]:

$$N_f = 2: \quad \hat{B}_K = 0.727(22)(12), \quad B_K^{\overline{\rm MS}}(2\,{\rm GeV}) = 0.531(16)(19) \quad \text{Ref. [70]}. \tag{161}$$

The result in the $\overline{\rm MS}$ scheme has been obtained by applying the same conversion factor of 1.369 as in the three-flavour theory.

Collaboration	Ref.	N_f	publication status	continuum extrapolation	chiral extrapolation	finite volume	renormalization	running	$B_K(\overline{\text{MS}}, 2\,\text{GeV})$	$\hat{B}_K$
ETM 15	[59]	2+1+1	A	★	○	○	★	*a*	0.524(13)(12)	0.717(18)(16)[1]
RBC/UKQCD 16	[71]	2+1	A	○	○	○	★	*b*	0.543(9)(13)[2]	0.744(13)(18)[3]
SWME 15A	[21]	2+1	A	★	○	★	○‡	–	0.537(4)(26)	0.735(5)(36)[4]
RBC/UKQCD 14B	[20]	2+1	A	★	★	★	★	*b*	0.5478(18)(110)[2]	0.7499(24)(150)
SWME 14	[19]	2+1	A	★	○	★	○‡	–	0.5388(34)(266)	0.7379(47)(365)
SWME 13A	[72]	2+1	A	★	○	★	○‡	–	0.537(7)(24)	0.735(10)(33)
SWME 13	[73]	2+1	C	★	○	★	○‡	–	0.539(3)(25)	0.738(5)(34)
RBC/UKQCD 12A	[18]	2+1	A	○	★	○	★	*b*	0.554(8)(14)[2]	0.758(11)(19)
Laiho 11	[17]	2+1	C	★	○	○	★	–	0.5572(28)(150)	0.7628(38)(205)[4]
SWME 11A	[74]	2+1	A	★	○	○	○‡	–	0.531(3)(27)	0.727(4)(38)
BMW 11	[22]	2+1	A	★	★	★	★	*c*	0.5644(59)(58)	0.7727(81)(84)
RBC/UKQCD 10B	[75]	2+1	A	○	○	★	★	*d*	0.549(5)(26)	0.749(7)(26)
SWME 10	[76]	2+1	A	★	○	○	○	–	0.529(9)(32)	0.724(12)(43)
Aubin 09	[77]	2+1	A	○	○	○	★	–	0.527(6)(21)	0.724(8)(29)

‡ The renormalization is performed using perturbation theory at 1-loop, with a conservative estimate of the uncertainty.

a B_K is renormalized nonperturbatively at scales $1/a \sim 2.2 - 3.3\,\text{GeV}$ in the $N_f = 4$ RI/MOM scheme using two different lattice momentum scale intervals, the first around $1/a$ while the second around 3.5 GeV. The impact of the two ways to the final result is taken into account in the error budget. Conversion to $\overline{\text{MS}}$ is at 1-loop at 3 GeV.

b B_K is renormalized nonperturbatively at a scale of 1.4 GeV in two RI/SMOM schemes for $N_f = 3$, and then run to 3 GeV using a nonperturbatively determined step-scaling function. Conversion to $\overline{\text{MS}}$ is at 1-loop order at 3 GeV.

c B_K is renormalized and run nonperturbatively to a scale of 3.5 GeV in the RI/MOM scheme. At the same scale conversion at 1-loop to $\overline{\text{MS}}$ is applied. Nonperturbative and NLO perturbative running agrees down to scales of 1.8 GeV within statistical uncertainties of about 2%.

d B_K is renormalized nonperturbatively at a scale of 2 GeV in two RI/SMOM schemes for $N_f = 3$, and then run to 3 GeV using a nonperturbatively determined step-scaling function. Conversion to $\overline{\text{MS}}$ is at 1-loop order at 3 GeV.

[1] $B_K(\overline{\text{MS}}, 2\,\text{GeV})$ and $\hat{B}_K$ are related using the conversion factor 1.369, i.e., the one obtained with $N_f = 2 + 1$.

[2] $B_K(\overline{\text{MS}}, 2\,\text{GeV})$ is obtained from the estimate for $\hat{B}_K$ using the conversion factor 1.369.

[3] $\hat{B}_K$ is obtained from $B_K(\overline{\text{MS}}, 3\,\text{GeV})$ using the conversion factor employed in Ref. [20].

[4] $\hat{B}_K$ is obtained from the estimate for $B_K(\overline{\text{MS}}, 2\,\text{GeV})$ using the conversion factor 1.369.

Table 31: Results for the kaon B-parameter in QCD with $N_f = 2 + 1 + 1$ and $N_f = 2 + 1$ dynamical flavours, together with a summary of systematic errors. Information about nonperturbative running is indicated in the column "running", with details given at the bottom of the table.

Collaboration	Ref.	N_f	publication status	continuum extrapolation	chiral extrapolation	finite volume	renormalization	running	$B_K(\overline{\text{MS}}, 2\,\text{GeV})$	$\hat{B}_K$
ETM 12D	[70]	2	A	★	○	○	★	*e*	0.531(16)(9)	0.727(22)(12)[1]
ETM 10A	[78]	2	A	★	○	○	★	*f*	0.533(18)(12)[1]	0.729(25)(17)

e B_K is renormalized nonperturbatively at scales $1/a \sim 2 - 3.7\,\text{GeV}$ in the $N_f = 2$ RI/MOM scheme. In this scheme, nonperturbative and NLO perturbative running are shown to agree from 4 GeV down to 2 GeV to better than 3% [78, 79].

f B_K is renormalized nonperturbatively at scales $1/a \sim 2 - 3\,\text{GeV}$ in the $N_f = 2$ RI/MOM scheme. In this scheme, nonperturbative and NLO perturbative running are shown to agree from 4 GeV down to 2 GeV to better than 3% [78, 79].

[1] $B_K(\overline{\text{MS}}, 2\,\text{GeV})$ and $\hat{B}_K$ are related using the conversion factor 1.369, i.e., the one obtained with $N_f = 2 + 1$.

Table 32: Results for the kaon B-parameter in QCD with $N_f = 2$ dynamical flavours, together with a summary of systematic errors. Information about nonperturbative running is indicated in the column "running", with details given at the bottom of the table.

6.4 Kaon BSM B-parameters

We now report on lattice results concerning the matrix elements of operators that encode the effects of physics beyond the Standard Model (BSM) to the mixing of neutral kaons. In this theoretical framework both the SM and BSM contributions add up to reproduce the experimentally observed value of ϵ_K. Since BSM contributions involve heavy but unobserved particles they are short-distance dominated. The effective Hamiltonian for generic $\Delta S = 2$ processes including BSM contributions reads

$$\mathcal{H}^{\Delta S=2}_{\text{eff,BSM}} = \sum_{i=1}^{5} C_i(\mu) Q_i(\mu), \tag{162}$$

where Q_1 is the four-quark operator of Eq. (139) that gives rise to the SM contribution to ϵ_K. In the so-called SUSY basis introduced by Gabbiani et al. [80] the operators $Q_2, \ldots, Q_5$ read [6]

$$\begin{aligned}
Q_2 &= \left(\bar{s}^a(1-\gamma_5)d^a\right)\left(\bar{s}^b(1-\gamma_5)d^b\right),\\
Q_3 &= \left(\bar{s}^a(1-\gamma_5)d^b\right)\left(\bar{s}^b(1-\gamma_5)d^a\right),\\
Q_4 &= \left(\bar{s}^a(1-\gamma_5)d^a\right)\left(\bar{s}^b(1+\gamma_5)d^b\right),\\
Q_5 &= \left(\bar{s}^a(1-\gamma_5)d^b\right)\left(\bar{s}^b(1+\gamma_5)d^a\right),
\end{aligned} \tag{163}$$

[6] Thanks to QCD parity invariance lattice computations for three more dimension-six operators, whose parity conserving parts coincide with the corresponding parity conserving contributions of the operators Q_1, Q_2 and Q_3, can be ignored.

where a and b denote colour indices. In analogy to the case of B_K one then defines the B-parameters of $Q_2, \ldots, Q_5$ according to

$$B_i(\mu) = \frac{\left\langle \bar{K}^0 \left| Q_i(\mu) \right| K^0 \right\rangle}{N_i \left\langle \bar{K}^0 \left| \bar{s}\gamma_5 d \right| 0 \right\rangle \left\langle 0 \left| \bar{s}\gamma_5 d \right| K^0 \right\rangle}, \quad i = 2, \ldots, 5. \tag{164}$$

The factors $\{N_2, \ldots, N_5\}$ are given by $\{-5/3, 1/3, 2, 2/3\}$, and it is understood that $B_i(\mu)$ is specified in some renormalization scheme, such as $\overline{\text{MS}}$ or a variant of the regularization-independent momentum subtraction (RI-MOM) scheme.

The SUSY basis has been adopted in Refs. [59, 70, 71, 81]. Alternatively, one can employ the chiral basis of Buras, Misiak and Urban [82]. The SWME collaboration prefers the latter since the anomalous dimension that enters the RG running has been calculated to 2-loops in perturbation theory [82]. Results obtained in the chiral basis can be easily converted to the SUSY basis via

$$B_3^{\text{SUSY}} = \tfrac{1}{2}\left(5B_2^{\text{chiral}} - 3B_3^{\text{chiral}}\right). \tag{165}$$

The remaining B-parameters are the same in both bases. In the following we adopt the SUSY basis and drop the superscript.

Older quenched results for the BSM B-parameters can be found in Refs. [83–85]. For a nonlattice approach to get estimates for the BSM B-parameters see Ref. [86].

Estimates for $B_2, \ldots, B_5$ have been reported for QCD with $N_f = 2$ (ETM 12D [70]), $N_f = 2+1$ (RBC/UKQCD 12E [81], SWME 13A [72], SWME 14C [87], SWME 15A [21], RBC/UKQCD 16 [71, 88]) and $N_f = 2+1+1$ (ETM 15 [59]) flavours of dynamical quarks. Since the publication of the FLAG 19 report [65] no new results for the BSM B-parameters have appeared in the bibliography. The available results are listed and compared in Tab. 33 and Fig. 21. In general one finds that the BSM B-parameters computed by different collaborations do not show the same level of consistency as the SM kaon-mixing parameter B_K discussed previously. Control over the systematic uncertainties from chiral and continuum extrapolations as well as finite-volume effects in $B_2, \ldots, B_5$ is expected to be at a commensurate level as for B_K, as far as the results by ETM 12D, ETM 15, SWME 15A and RBC/UKQCD 16 are concerned, since the set of gauge ensembles employed in both kinds of computations is the same. The calculation by RBC/UKQCD 12E has been performed at a single value of the lattice spacing and a minimum pion mass of 290 MeV.

Let us notice that as reported in RBC/UKQCD 16 [71] the comparison of results obtained in the conventional RI-MOM and two RI-SMOM schemes shows significant discrepancies for B_4 and B_5 in the $\overline{\text{MS}}$ scheme at the scale of 3 GeV, which amount up to 2.8σ in the case of B_5. By contrast, the agreement for B_2 and B_3 determined for different intermediate scheme is much better. The RBC/UKQCD collaboration has presented an ongoing study [89] in which simulations with two values of the lattice spacing at the physical point and with a third finer lattice spacing at $M_\pi = 234$ MeV are employed in order to obtain the BSM matrix elements in the continuum limit. Results are still preliminary.

The findings by RBC/UKQCD 16 [71, 88] provide evidence that the nonperturbative determination of the matching factors depends strongly on the details of the implementation of the Rome-Southampton method. The use of nonexceptional momentum configurations in the calculation of the vertex functions produces a significant modification of the renormalization factors, which affects the matching between $\overline{\text{MS}}$ and the intermediate momentum subtraction scheme. This effect is most pronounced in B_4 and B_5. Furthermore, it can be noticed that the estimates for B_4 and B_5 from RBC/UKQCD 16 are much closer to those of SWME

15A. At the same time, the results for B_2 and B_3 obtained by ETM 15, SWME 15A and RBC/UKQCD 16 are in good agreement within errors.

Collaboration	Ref.	N_f	publication status	continuum extrapolation	chiral extrapolation	finite volume	renormalization	running	B_2	B_3	B_4	B_5
ETM 15	[59]	2+1+1	A	★	○	○	★	*a*	0.46(1)(3)	0.79(2)(5)	0.78(2)(4)	0.49(3)(3)
RBC/UKQCD 16	[71]	2+1	A	○	○	○	★	*b*	0.488(7)(17)	0.743(14)(65)	0.920(12)(16)	0.707(8)(44)
SWME 15A	[21]	2+1	A	★	○	★	○†	–	0.525(1)(23)	0.773(6)(35)	0.981(3)(62)	0.751(7)(68)
SWME 14C	[87]	2+1	C	★	○	★	○†	–	0.525(1)(23)	0.774(6)(64)	0.981(3)(61)	0.748(9)(79)
SWME 13A‡	[72]	2+1	A	★	○	★	○†	–	0.549(3)(28)	0.790(30)	1.033(6)(46)	0.855(6)(43)
RBC/ UKQCD 12E	[81]	2+1	A	■	○	★	★	*b*	0.43(1)(5)	0.75(2)(9)	0.69(1)(7)	0.47(1)(6)
ETM 12D	[70]	2	A	★	○	○	★	*c*	0.47(2)(1)	0.78(4)(2)	0.76(2)(2)	0.58(2)(2)

† The renormalization is performed using perturbation theory at 1-loop, with a conservative estimate of the uncertainty.

a B_i are renormalized nonperturbatively at scales $1/a \sim 2.2 - 3.3\,\text{GeV}$ in the $N_f = 4$ RI/MOM scheme using two different lattice momentum scale intervals, with values around $1/a$ for the first and around 3.5 GeV for the second one. The impact of these two ways to the final result is taken into account in the error budget. Conversion to $\overline{\text{MS}}$ is at 1-loop at 3 GeV.

b The B-parameters are renormalized nonperturbatively at a scale of 3 GeV.

c B_i are renormalized nonperturbatively at scales $1/a \sim 2 - 3.7\,\text{GeV}$ in the $N_f = 2$ RI/MOM scheme using two different lattice momentum scale intervals, with values around $1/a$ for the first and around 3 GeV for the second one.

‡ The computation of B_4 and B_5 has been revised in Refs. [21] and [87].

Table 33: Results for the BSM B-parameters $B_2, \ldots, B_5$ in the $\overline{\text{MS}}$ scheme at a reference scale of 3 GeV. Information about nonperturbative running is indicated in the column "running", with details given at the bottom of the table.

A nonperturbative computation of the running of the four-fermion operators contributing to the B_2, ..., B_5 parameters has been carried out with two dynamical flavours using the Schrödinger functional renormalization scheme [24]. Renormalization matrices of the operator basis are used to build step-scaling functions governing the continuum-limit running between hadronic and electroweak scales. A comparison to perturbative results using NLO (2-loops) for the four-fermion operator anomalous dimensions indicates that, at scales of about 3 GeV, nonperturbative effects can induce a sizeable contribution to the running.

A detailed look at the calculations reported in the works of ETM 15 [59], SWME 15A [21] and RBC/UKQCD 16 [71] reveals that cutoff effects appear to be larger for the BSM B-parameters compared to B_K. Depending on the details of the renormalization procedure and/or the fit ansatz for the combined chiral and continuum extrapolation, the results obtained at the coarsest lattice spacing differ by 15–30%. At the same time the available range of lattice spacings is typically much reduced compared to the corresponding calculations of B_K, as can be seen by comparing the quality criteria in Tabs. 31 and 33. Hence, the impact of the renormalization procedure and the continuum limit on the BSM B-parameters certainly requires further investigation.

Finally we present our estimates for the BSM B-parameters, quoted in the $\overline{\text{MS}}$-scheme at scale 3 GeV. For $N_f = 2+1$ our estimate is given by the average between the results from SWME 15A and RBC/UKQCD 16, i.e.,

$$N_f = 2+1: \tag{166}$$
$$B_2 = 0.502(14), \quad B_3 = 0.766(32), \quad B_4 = 0.926(19), \quad B_5 = 0.720(38), \quad \text{Refs. [21, 71]}.$$

For $N_f = 2+1+1$ and $N_f = 2$, our estimates coincide with the ones by ETM 15 and ETM 12D, respectively, since there is only one computation for each case. Thus we quote

$$N_f = 2+1+1: \tag{167}$$
$$B_2 = 0.46(1)(3), \quad B_3 = 0.79(2)(5), \quad B_4 = 0.78(2)(4), \quad B_5 = 0.49(3)(3), \quad \text{Ref. [59]},$$

$$N_f = 2: \tag{168}$$
$$B_2 = 0.47(2)(1), \quad B_3 = 0.78(4)(2), \quad B_4 = 0.76(2)(2), \quad B_5 = 0.58(2)(2), \quad \text{Ref. [70]}.$$

Based on the above discussion on the effects of employing different intermediate momentum subtraction schemes in the nonperturbative renormalization of the operators, the discrepancy for B_4 and B_5 results between $N_f = 2, 2+1+1$ and $N_f = 2+1$ computations should not be considered an effect associated with the number of dynamical flavours. To clarify the present situation, it would be important to perform a direct comparison of results by the ETM collaboration obtained both with RI-MOM and RI-SMOM methods. Furthermore, extending the computation of the BSM-B parameters to include physical point simulations with improved continuum-limit extrapolations would also provide valuable information. As a closing remark, we encourage authors to provide the correlation matrix of the B_i parameters since this information is required in phenomenological studies of New Physics scenarios.

References

[1] G.C. Branco, L. Lavoura and J.P. Silva, *CP violation*, *Int. Ser. Monogr. Phys.* **103** (1999) 1.

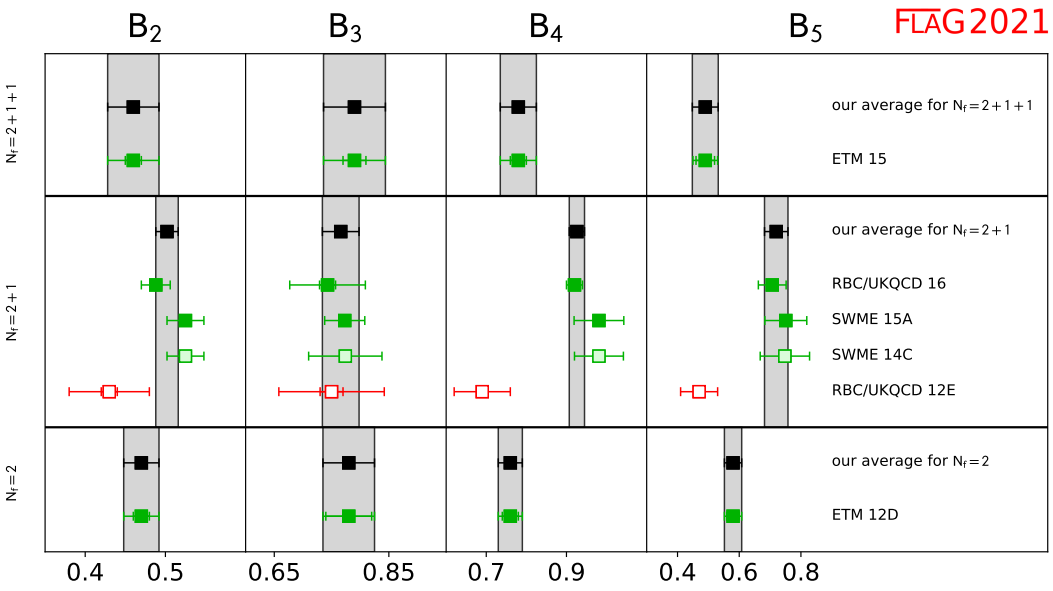

Figure 21: Lattice results for the BSM B-parameters defined in the $\overline{\text{MS}}$ scheme at a reference scale of 3 GeV, see Tab. 33.

[2] M. Sozzi, *Discrete Symmetries and CP Violation: From Experiment to Theory*, *Oxford University Press* (2008) 1.

[3] A. Buras, *Gauge Theories of Weak Decays*, *Cambridge University Press* (2020) 1.

[4] G. Buchalla, A.J. Buras and M.E. Lautenbacher, *Weak decays beyond leading logarithms*, *Rev. Mod. Phys.* **68** (1996) 1125 [hep-ph/9512380].

[5] A.J. Buras, *Weak Hamiltonian, CP violation and rare decays*, hep-ph/9806471, Published in *Les Houches 1997, Probing the standard model of particle interactions*, Pt. 1, 281-539.

[6] L. Lellouch, *Flavor physics and lattice quantum chromodynamics*, in *Modern perspectives in lattice QCD: Quantum field theory and high performance computing. Proceedings, International School, 93rd Session, Les Houches, France, August 3-28, 2009*, pp. 629–698, 2011 [1104.5484].

[7] K. Anikeev et al., *B physics at the Tevatron: Run II and beyond*, hep-ph/0201071.

[8] U. Nierste, *Three lectures on meson mixing and CKM phenomenology, published in Dubna 2008, Heavy Quark Physics (HQP08), pp. 1-39*, 0904.1869.

[9] A.J. Buras and D. Guadagnoli, *Correlations among new CP violating effects in $\Delta F = 2$ observables*, *Phys. Rev.* **D78** (2008) 033005 [0805.3887].

[10] A.J. Buras, D. Guadagnoli and G. Isidori, *On ϵ_K beyond lowest order in the operator product expansion*, *Phys. Lett.* **B688** (2010) 309 [1002.3612].

[11] Particle Data Group collaboration, *Review of Particle Physics*, *PTEP* **2020** (2020) 083C01.

[12] T. Inami and C.S. Lim, *Effects of superheavy quarks and leptons in low-energy weak processes $K_L \to \mu\bar{\mu}$, $K^+ \to \pi^+\nu\bar{\nu}$ and $K^0 \leftrightarrow \bar{K}^0$*, *Prog. Theor. Phys.* **65** (1981) 297.

[13] J. Brod and M. Gorbahn, *Next-to-next-to-leading-order charm-quark contribution to the CP violation parameter ϵ_K and ΔM_K*, *Phys.Rev.Lett.* **108** (2012) 121801 [1108.2036].

[14] J. Brod and M. Gorbahn, *ϵ_K at next-to-next-to-leading order: the charm-top-quark contribution*, *Phys. Rev.* **D82** (2010) 094026 [1007.0684].

[15] G. Martinelli, C. Pittori, C.T. Sachrajda, M. Testa and A. Vladikas, *A general method for nonperturbative renormalization of lattice operators*, *Nucl. Phys.* **B445** (1995) 81 [hep-lat/9411010].

[16] M. Lüscher, R. Narayanan, P. Weisz and U. Wolff, *The Schrödinger functional: a renormalizable probe for non-abelian gauge theories*, *Nucl. Phys.* **B384** (1992) 168 [hep-lat/9207009].

[17] J. Laiho and R.S. Van de Water, *Pseudoscalar decay constants, light-quark masses and B_K from mixed-action lattice QCD*, *PoS* **LATTICE2011** (2011) 293 [1112.4861].

[18] [RBC/UKQCD 12] R. Arthur et al., *Domain wall QCD with near-physical pions*, *Phys.Rev.* **D87** (2013) 094514 [1208.4412].

[19] [SWME 14] T. Bae et al., *Improved determination of B_K with staggered quarks*, *Phys. Rev.* **D89** (2014) 074504 [1402.0048].

[20] [RBC/UKQCD 14B] T. Blum et al., *Domain wall QCD with physical quark masses*, *Phys. Rev.* **D93** (2016) 074505 [1411.7017].

[21] [SWME 15A] Y.-C. Jang et al., *Kaon BSM B-parameters using improved staggered fermions from $N_f = 2{+}1$ unquenched QCD*, *Phys. Rev.* **D93** (2016) 014511 [1509.00592].

[22] [BMW 11] S. Dürr, Z. Fodor, C. Hoelbling, S. Katz, S. Krieg et al., *Precision computation of the kaon bag parameter*, *Phys.Lett.* **B705** (2011) 477 [1106.3230].

[23] [ALPHA 07A] P. Dimopoulos et al., *Non-perturbative renormalisation of $\Delta F = 2$ four-fermion operators in two-flavour QCD*, *JHEP* **0805** (2008) 065 [0712.2429].

[24] [ALPHA 18B] P. Dimopoulos et al., *Non-Perturbative Renormalisation and Running of BSM Four-Quark Operators in $N_f = 2$ QCD*, *Eur. Phys. J.* **C78** (2018) 579 [1801.09455].

[25] [RBC/UKQCD 12F] N. H. Christ, T. Izubuchi, C.T. Sachrajda, A. Soni and J. Yu, *Long distance contribution to the KL-KS mass difference*, *Phys. Rev.* **D88** (2013) 014508 [1212.5931].

[26] J. Brod, M. Gorbahn and E. Stamou, *Standard-model prediction of ϵ_K with manifest CKM unitarity*, *Phys. Rev. Lett.* **125** (2020) 171803 [1911.06822].

[27] V. Cirigliano, A. Pich, G. Ecker and H. Neufeld, *Isospin violation in epsilon-prime*, *Phys. Rev. Lett.* **91** (2003) 162001 [hep-ph/0307030].

[28] V. Cirigliano, H. Gisbert, A. Pich and A. Rodríguez-Sánchez, *Isospin-violating contributions to ϵ'/ϵ*, *JHEP* **02** (2020) 032 [1911.01359].

[29] [RBC/UKQCD 20] R. Abbott et al., *Direct CP violation and the $\Delta I = 1/2$ rule in $K \to \pi\pi$ decay from the Standard Model*, *Phys. Rev. D* **102** (2020) 054509 [2004.09440].

[30] [RBC/UKQCD 15G] Z. Bai et al., *Standard Model Prediction for Direct CP Violation in $K \to \pi\pi$ Decay*, *Phys. Rev. Lett.* **115** (2015) 212001 [1505.07863].

[31] [RBC/UKQCD 15F] T. Blum et al., *$K \to \pi\pi$ $\Delta I = 3/2$ decay amplitude in the continuum limit*, *Phys. Rev.* **D91** (2015) 074502 [1502.00263].

[32] Particle Data Group collaboration, *Review of Particle Physics*, *Phys. Rev.* **D98** (2018) 030001.

[33] Z. Bai, *Long distance part of ϵ_K from lattice QCD*, *PoS* **LATTICE2016** (2017) 309 [1611.06601].

[34] Z. Bai, N.H. Christ, T. Izubuchi, C.T. Sachrajda, A. Soni and J. Yu, *$K_L - K_S$ Mass Difference from Lattice QCD*, *Phys. Rev. Lett.* **113** (2014) 112003 [1406.0916].

[35] N.H. Christ, X. Feng, G. Martinelli and C.T. Sachrajda, *Effects of finite volume on the KL-KS mass difference*, *Phys. Rev.* **D91** (2015) 114510 [1504.01170].

[36] B. Wang, *Calculation of the $K_L - K_S$ mass difference for physical quark masses*, *PoS* **LATTICE2019** (2019) 093 [2001.06374].

[37] Z. Bai et al., *Erratum: Standard-Model Prediction for Direct CP Violation in $K \to \pi\pi$ Decay*, 1603.03065.

[38] M. Gaillard and B.W. Lee, *Δ $I = 1/2$ Rule for Nonleptonic Decays in Asymptotically Free Field Theories*, *Phys. Rev. Lett.* **33** (1974) 108.

[39] G. Altarelli and L. Maiani, *Octet Enhancement of Nonleptonic Weak Interactions in Asymptotically Free Gauge Theories*, *Phys. Lett. B* **52** (1974) 351.

[40] [RBC/UKQCD 21] T. Blum et al., *Lattice determination of $I = 0$ and 2 $\pi\pi$ scattering phase shifts with a physical pion mass*, *Phys. Rev. D* **104** (2021) 114506 [2103.15131].

[41] N. Ishizuka, K.I. Ishikawa, A. Ukawa and T. Yoshié, *Calculation of $K \to \pi\pi$ decay amplitudes with improved Wilson fermion action in lattice QCD*, *Phys. Rev.* **D92** (2015) 074503 [1505.05289].

[42] N. Ishizuka, K.I. Ishikawa, A. Ukawa and T. Yoshié, *Calculation of $K \to \pi\pi$ decay amplitudes with improved Wilson fermion action in non-zero momentum frame in lattice QCD*, *Phys. Rev.* **D98** (2018) 114512 [1809.03893].

[43] A. Donini, P. Hernández, C. Pena and F. Romero-López, *Nonleptonic kaon decays at large N_c*, *Phys. Rev.* **D94** (2016) 114511 [1607.03262].

[44] A. Donini, P. Hernández, C. Pena and F. Romero-López, *Dissecting the $\Delta I = 1/2$ rule at large N_c*, *Eur. Phys. J. C* **80** (2020) 638 [2003.10293].

[45] N. Christ and X. Feng, *Including electromagnetism in $K \to \pi\pi$ decay calculations*, *EPJ Web Conf.* **175** (2018) 13016 [1711.09339].

[46] Y. Cai and Z. Davoudi, *QED-corrected Lellouch-Luescher formula for $K \to \pi\pi$ decay*, *PoS* **LATTICE2018** (2018) 280 [1812.11015].

[47] [SWME 15B] J. A. Bailey, Y.-C. Jang, W. Lee and S. Park, *Standard Model evaluation of ε_K using lattice QCD inputs for $\hat{B}_K$ and V_{cb}*, *Phys. Rev.* **D92** (2015) 034510 [1503.05388].

[48] J.A. Bailey, S. Lee, W. Lee, J. Leem and S. Park, *Updated evaluation of ϵ_K in the standard model with lattice QCD inputs*, *Phys. Rev.* **D98** (2018) 094505 [1808.09657].

[49] [LANL-SWME 19] J. Kim, S. Lee, W. Lee, Y.-C. Jang, J. Leem and S. Park, *2019 update of ε_K with lattice QCD inputs*, *PoS* **LATTICE2019** (2019) 029 [1912.03024].

[50] D. Bećirević et al., *$K^0\bar{K}^0$ mixing with Wilson fermions without subtractions*, *Phys. Lett.* **B487** (2000) 74 [hep-lat/0005013].

[51] [ALPHA 01] R. Frezzotti, P.A. Grassi, S. Sint and P. Weisz, *Lattice QCD with a chirally twisted mass term*, *JHEP* **08** (2001) 058 [hep-lat/0101001].

[52] [ALPHA 06] P. Dimopoulos et al., *A precise determination of B_K in quenched QCD*, *Nucl. Phys.* **B749** (2006) 69 [hep-ph/0601002].

[53] [ALPHA 07] P. Dimopoulos et al., *Flavour symmetry restoration and kaon weak matrix elements in quenched twisted mass QCD*, *Nucl. Phys.* **B776** (2007) 258 [hep-lat/0702017].

[54] R.S. Van de Water and S.R. Sharpe, *B_K in staggered chiral perturbation theory*, *Phys. Rev.* **D73** (2006) 014003 [hep-lat/0507012].

[55] J.A. Bailey, H.-J. Kim, W. Lee and S.R. Sharpe, *Kaon mixing matrix elements from beyond-the-Standard-Model operators in staggered chiral perturbation theory*, *Phys. Rev.* **D85** (2012) 074507 [1202.1570].

[56] P.H. Ginsparg and K.G. Wilson, *A remnant of chiral symmetry on the lattice*, *Phys. Rev.* **D25** (1982) 2649.

[57] Y. Aoki et al., *The Kaon B-parameter from quenched domain-wall QCD*, *Phys. Rev. D* **73** (2006) 094507 [hep-lat/0508011].

[58] [RBC/UKQCD] N. Christ, *Estimating domain wall fermion chiral symmetry breaking*, *PoS* **LAT2005** (2006) 345.

[59] [ETM 15] N. Carrasco, P. Dimopoulos, R. Frezzotti, V. Lubicz, G.C. Rossi, S. Simula et al., $\Delta S = 2$ *and* $\Delta C = 2$ *bag parameters in the standard model and beyond from* $N_f = 2+1+1$ *twisted-mass lattice QCD*, *Phys. Rev.* **D92** (2015) 034516 [1505.06639].

[60] V. Cirigliano, J.F. Donoghue and E. Golowich, *Dimension eight operators in the weak OPE*, *JHEP* **10** (2000) 048 [hep-ph/0007196].

[61] A.J. Buras, M. Jamin and P.H. Weisz, *Leading and next-to-leading QCD corrections to* ϵ *parameter and* $B_0 - \bar{B}_0$ *mixing in the presence of a heavy top quark*, *Nucl. Phys.* **B347** (1990) 491.

[62] [ALPHA 20] R. Höllwieser, F. Knechtli and T. Korzec, *Scale setting for* $N_f = 3+1$ *QCD*, *Eur. Phys. J. C* **80** (2020) 349 [2002.02866].

[63] [ALPHA 14A] M. Bruno, J. Finkenrath, F. Knechtli, B. Leder and R. Sommer, *Effects of Heavy Sea Quarks at Low Energies*, *Phys. Rev. Lett.* **114** (2015) 102001 [1410.8374].

[64] A. Athenodorou, J. Finkenrath, F. Knechtli, T. Korzec, B. Leder, M.K. Marinkovic et al., *How perturbative are heavy sea quarks?*, *Nucl. Phys.* **B943** (2019) 114612 [1809.03383].

[65] [FLAG 19] S. Aoki et al., *FLAG Review 2019: Flavour Lattice Averaging Group (FLAG)*, *Eur. Phys. J. C* **80** (2020) 113 [1902.08191].

[66] [FLAG 16] S. Aoki et al., *Review of lattice results concerning low-energy particle physics*, *Eur. Phys. J.* **C77** (2017) 112 [1607.00299].

[67] [FLAG 13] S. Aoki, Y. Aoki, C. Bernard, T. Blum, G. Colangelo et al., *Review of lattice results concerning low-energy particle physics*, *Eur.Phys.J.* **C74** (2014) 2890 [1310.8555].

[68] A. Suzuki, Y. Taniguchi, H. Suzuki and K. Kanaya, *Four quark operators for kaon bag parameter with gradient flow*, *Phys. Rev. D* **102** (2020) 034508 [2006.06999].

[69] M. Schmelling, *Averaging correlated data*, *Phys.Scripta* **51** (1995) 676.

[70] [ETM 12D] V. Bertone et al., *Kaon Mixing Beyond the SM from* N_f*=2 tmQCD and model independent constraints from the UTA*, *JHEP* **03** (2013) 089 [1207.1287], [Erratum: JHEP07,143(2013)].

[71] [RBC/UKQCD 16] N. Garron, R.J. Hudspith and A.T. Lytle, *Neutral Kaon Mixing Beyond the Standard Model with* $n_f = 2+1$ *Chiral Fermions Part 1: Bare Matrix Elements and Physical Results*, *JHEP* **11** (2016) 001 [1609.03334].

[72] [SWME 13A] T. Bae et al., *Neutral kaon mixing from new physics: matrix elements in* $N_f = 2+1$ *lattice QCD*, *Phys. Rev.* **D88** (2013) 071503 [1309.2040].

[73] [SWME 13] T. Bae et al., *Update on* B_K *and* ε_K *with staggered quarks*, *PoS* **LATTICE2013** (2013) 476 [1310.7319].

[74] [SWME 11A] T. Bae et al., *Kaon B-parameter from improved staggered fermions in $N_f = 2+1$ QCD*, *Phys.Rev.Lett.* **109** (2012) 041601 [1111.5698].

[75] [RBC/UKQCD 10B] Y. Aoki et al., *Continuum limit of B_K from 2+1 flavor domain wall QCD*, *Phys.Rev.* **D84** (2011) 014503 [1012.4178].

[76] [SWME 10] T. Bae et al., *B_K using HYP-smeared staggered fermions in $N_f = 2+1$ unquenched QCD*, *Phys. Rev.* **D82** (2010) 114509 [1008.5179].

[77] C. Aubin, J. Laiho and R.S. Van de Water, *The neutral kaon mixing parameter B_K from unquenched mixed-action lattice QCD*, *Phys. Rev.* **D81** (2010) 014507 [0905.3947].

[78] [ETM 10A] M. Constantinou et al., *BK-parameter from $N_f = 2$ twisted mass lattice QCD*, *Phys. Rev.* **D83** (2011) 014505 [1009.5606].

[79] [ETM 10C] M. Constantinou et al., *Non-perturbative renormalization of quark bilinear operators with $N_f = 2$ (tmQCD) Wilson fermions and the tree- level improved gauge action*, *JHEP* **08** (2010) 068 [1004.1115].

[80] F. Gabbiani, E. Gabrielli, A. Masiero and L. Silvestrini, *A Complete analysis of FCNC and CP constraints in general SUSY extensions of the standard model*, *Nucl. Phys.* **B477** (1996) 321 [hep-ph/9604387].

[81] [RBC/UKQCD 12E] P. A. Boyle, N. Garron and R.J. Hudspith, *Neutral kaon mixing beyond the standard model with $n_f = 2+1$ chiral fermions*, *Phys. Rev.* **D86** (2012) 054028 [1206.5737].

[82] A.J. Buras, M. Misiak and J. Urban, *Two loop QCD anomalous dimensions of flavor changing four quark operators within and beyond the standard model*, *Nucl. Phys.* **B586** (2000) 397 [hep-ph/0005183].

[83] C.R. Allton, L. Conti, A. Donini, V. Gimenez, L. Giusti, G. Martinelli et al., *B parameters for Delta S = 2 supersymmetric operators*, *Phys. Lett.* **B453** (1999) 30 [hep-lat/9806016].

[84] A. Donini, V. Gimenez, L. Giusti and G. Martinelli, *Renormalization group invariant matrix elements of Delta S = 2 and Delta I = 3/2 four fermion operators without quark masses*, *Phys. Lett.* **B470** (1999) 233 [hep-lat/9910017].

[85] R. Babich, N. Garron, C. Hoelbling, J. Howard, L. Lellouch and C. Rebbi, *K0 – anti-K0 mixing beyond the standard model and CP-violating electroweak penguins in quenched QCD with exact chiral symmetry*, *Phys. Rev.* **D74** (2006) 073009 [hep-lat/0605016].

[86] A.J. Buras and J.-M. Gérard, *Dual QCD Insight into BSM Hadronic Matrix Elements for $K^0 - \bar{K}^0$ Mixing from Lattice QCD*, *Acta Phys. Polon.* **B50** (2019) 121 [1804.02401].

[87] [SWME 14C] J. Leem et al., *Calculation of BSM Kaon B-parameters using Staggered Quarks*, *PoS* **LATTICE2014** (2014) 370 [1411.1501].

[88] [RBC/UKQCD 17A] P. Boyle et al., *Neutral kaon mixing beyond the Standard Model with $n_f = 2+1$ chiral fermions. Part 2: non perturbative renormalisation of the $\Delta F = 2$ four-quark operators*, *JHEP* **10** (2017) 054 [1708.03552].

[89] P. Boyle, N. Garron, R.J. Hudspith, A. Juttner, J. Kettle, A. Khamseh et al., *Beyond the Standard Model Kaon Mixing with Physical Masses*, in *Proceedings, 36th International Symposium on Lattice Field Theory (Lattice 2018): East Lansing, MI, United States, July 22-28, 2018*, vol. LATTICE2018, p. 285, 2019, DOI [1812.04981].